Tradeoff between Contrail Reduction and Emissions in United States National Airspace

Neil Y. Chen* and Banavar Sridhar†

NASA Ames Research Center, Moffett Field, CA 94035-1000

Hok K. Ng‡

University of California, Santa Cruz, Moffett Field, CA 94035-1000

This paper describes a class of strategies for reducing persistent contrail formation with the capability of trading off between contrails and aircraft induced emissions. The concept of contrail frequency index is defined and used to quantify the contrail activities. The contrail reduction strategies reduce the contrail frequency index by altering aircraft's cruising altitude with consideration to extra emissions. The strategies use a user-defined factor to trade off between contrail reduction and extra emissions. The analysis shows that contrails can be reduced with extra emissions and without adding congestion to airspace. For a day with high contrail activities, the results show that the maximal contrail reduction strategy can achieve a contrail reduction of 88%. When a trade-off factor is used, the strategy can achieve less contrail reduction while emitting less emissions compared to the maximal contrail reduction strategy. The user-defined trade-off factor provides a flexible way to trade off between contrail reduction and extra emissions. Better understanding of the trade-offs between contrails and emissions and their impact on the climate need to be developed to fully utilize this class of contrail reduction strategies. The strategies provide a starting point for developing operational policies to reduce the impact of aviation on climate.

I. Introduction

Aircraft induced environmental impact has drawn attention in recent years.[1] The three largest emission impacts include direct emissions of greenhouse gases such as CO_2, emissions of NOx, and persistent contrails. Contrails are clouds that are visible trails of water vapor made by the exhaust of aircraft engines. Contrails form when a mixture of warm engine exhaust gases and cold ambient air reaches saturation with respect to water, forming liquid drops which quickly freeze. They persist if the aircraft is flying in certain atmospheric conditions. Persistent contrails reduce incoming solar radiation and outgoing thermal radiation in a way that accumulates heat.[2] The global mean contrail cover in 1992 was estimated to double by 2015, and quadruple by 2050 due to an increase in air traffic.[3] Studies suggest that the environmental impact from persistent contrail is estimated to be three to four times,[4] or even ten times[5] larger than the aviation induced emissions. Therefore, methods to reduce aircraft induced persistent contrails are needed to minimize the impact of aviation on climate.

Efforts have been made in the past to reduce the persistent contrail formation. Gierens[6] and Noppel[7] reviewed various strategies for contrail avoidance. Mannstein[8] proposed a strategy to reduce the climate impact of contrails significantly by only small changes in individual flight altitude. Campbell[9] presented a methodology to optimally reroute aircraft trajectories to avoid the formation of persistent contrails with the use of mixed integer programming. Both methodologies require onboard contrail detection system and flight rerouting. Fichter[10] showed that the global annual mean contrail coverage could be reduced by downshifting the cruise altitude. Williams[11,12] proposed strategies for contrail reduction by identifying fixed and varying

*Research Aerospace Engineer, Systems Modeling and Optimization branch, MS 210-10, Senior Member.

†Senior Scientist for Air Transportation Systems, Aviation Systems Division, MS 210-10, Fellow.

‡Senior Software Engineer, University Affiliated Research Center, MS 210-8, Member.

maximum altitude restriction policy. These restrictions generally imply more fuel burn, thus more emissions, and add congestion to the already crowded airspace at lower altitudes.

The objective of this paper is to develop strategies to reduce persistent contrail formation with consideration to extra emissions and air space congestion. The concept of contrail frequency index is used to quantify the severity of contrail formation. The strategy for reducing persistent contrail formation is to reduce contrail frequency index by altering the aircraft's cruising altitude with minimal increase in emissions. A class of contrail reduction strategies that considers extra emissions is proposed. It provides a flexible way to trade off between contrail reduction and emissions. The results show that the contrail frequency index can be reduced with extra emissions and without adding congestion to airspace. The strategies provide a starting point for developing operational policies to reduce the impact of aviation on climate.

The remainder of the paper is organized as follows. Section II provides descriptions of contrail model, definition of contrail frequency index, and the fuel burn and emission models. Next, contrail reduction strategies and the trade-offs between contrail reduction and emissions are described in Section III. Section IV shows the results. Finally, Section V presents a summary and conclusions.

II. Data and Model

II.A. Contrail Model

Contrails are vapor trails caused by aircraft operating at high altitudes under certain atmospheric conditions. The contrail model in this paper uses atmospheric temperature and humidity data retrieved from the Rapid Updated Cycle (RUC) data, provided by the National Oceanic and Atmospheric Administration (NOAA). The horizontal resolution in RUC is 13-km. RUC data has 37 vertical isobaric pressure levels ranging between 100 and 1000 millibar (mb) in 25 mb increments. Since the vertical isobaric pressure levels do not correspond with 2,000 feet increments, linear interpolation was used to convert the RUC data to a vertical range from 26,000 feet to 44,000 feet with an increment of 2,000 feet. This range is chosen because it generally is too warm for contrails to form below 26,000 feet and most aircraft fly below 44,000 feet.

Contrails form when a mixture of warm engine exhaust gases and cold ambient air reaches saturation with respect to water, forming liquid drops which quickly freeze. Contrails form in the regions of airspace that have ambient Relative Humidity with respect to Water (RHw) greater than a critical value r_{contr}.[13] Regions with RHw greater than or equal to 100% are excluded because clouds are already present.[14] Contrails can persist when the environmental Relative Humidity with respect to Ice (RHi) is greater than 100%.[15] In this paper, contrail favorable regions are defined as the regions of airspace that have $r_{contr} \leq RHw < 100\%$ and $RHi \geq 100\%$.

The estimated critical relative humidity for contrail formation at a given temperature T (in Celsius) can be calculated as

$$r_{contr} = \frac{G(T - T_{contr}) + e_{sat}^{liq}(T_{contr})}{e_{sat}^{liq}(T)}, \tag{1}$$

where $e_{sat}^{liq}(T)$ is the saturation vapor pressure over water at a given temperature. The estimated threshold temperature for contrail formation at liquid saturation is

$$T_{contr} = -46.46 + 9.43\ln(G - 0.053) + 0.72\ln^2(G - 0.053), \tag{2}$$

where

$$G = \frac{EI_{H_2O} C_p P}{\epsilon Q(1 - \eta)}, \tag{3}$$

EI_{H_2O} is the emission index of water vapor (assumed to be 1.25); $C_p = 1004$ (in $JKg^{-1}K^{-1}$) is the isobaric heat capacity of air, P (in Pa) is the ambient air pressure, $\epsilon = 0.6222$ is the ratio of molecular masses of water and dry air, $Q = 43 \cdot 10^6$ (in JKg^{-1}) is the specific combustion heat, and $\eta = 0.3$ is the average propulsion efficiency of the jet engine. The value of r_{contr} is computed by Eq (1)-(3) using RUC measurements for RHw and temperatures. RHi is calculated by temperature and relative humidity using the following formula:[16]

$$RHi = RHw \cdot \frac{6.0612 e^{18.102T/(249.52+T)}}{6.1162 e^{22.577T/(237.78+T)}}, \tag{4}$$

where T is the temperature in Celsius. Figure 1 shows the temperature, RHw, RHi, and contrail favorable regions at 8AM EDT on April 23, 2010 at an altitude of 34,000 feet.

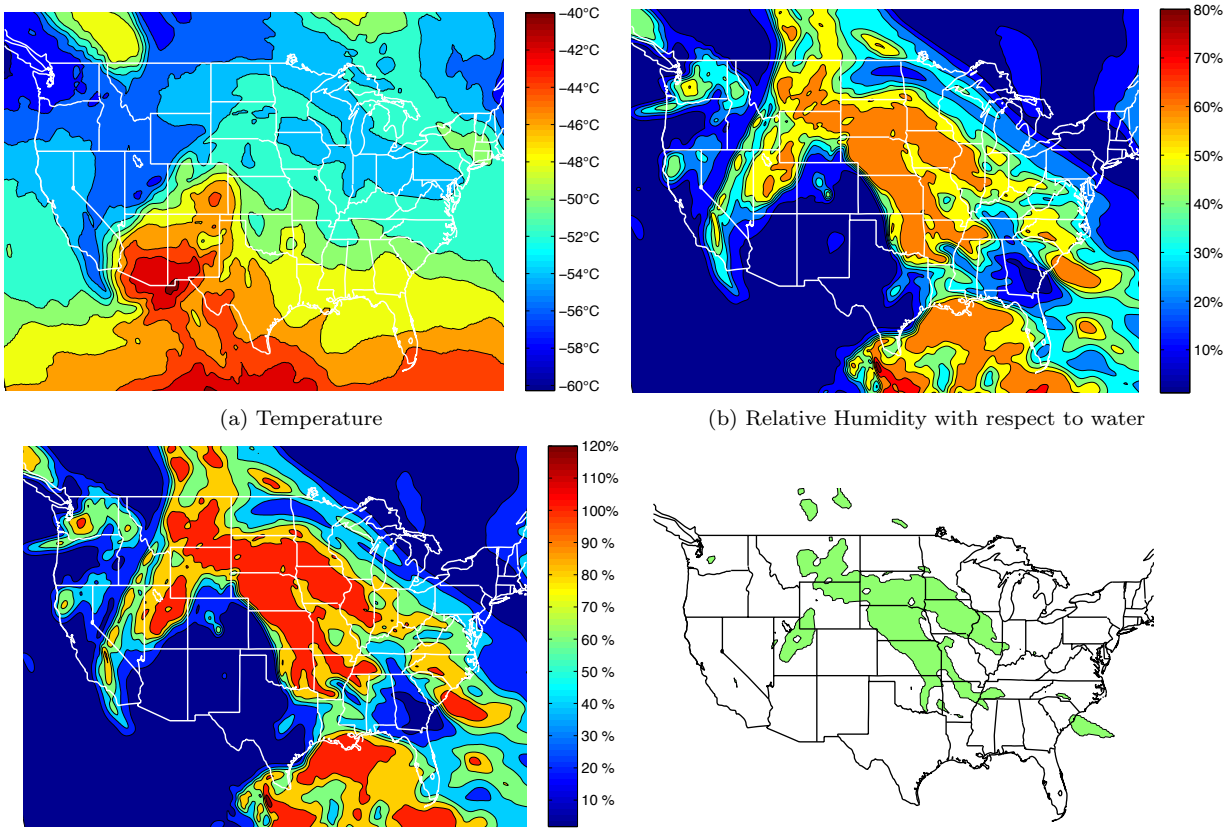

(a) Temperature

(b) Relative Humidity with respect to water

(c) Relative Humidity with respect to ice

(d) Contrail favorable regions

Figure 1. Atmospheric data and contrail favorable regions at 34,000 feet at 8AM EDT on April 23, 2010.

II.B. Contrail Frequency Index

Contrail frequency index (CFI) is used to quantify the severity of contrail activities. This paper uses 13km RUC data instead of the 40km RUC data used in Ref. 17. The modified 13km RUC data divide the U.S. national airspace into a three dimensional grid with 337 elements along the latitude, 451 elements along the longitude, and 10 altitudes ranging from 26,000 feet to 44,000 feet. Air traffic in the U.S. can be mapped into the same volumetric grid. Contrail frequency index is the number of aircraft in a volumetric element which meets conditions for persistent contrail formation. Contrail frequency index is zero for volumetric elements which do not meet the conditions for persistent contrail formation. Precise definitions of contrail frequency index are provided by the following equations.

The altitude level index l is defined as $l = 1 \ldots 10$ corresponding to altitudes of $26,000$, $28,000$, $\ldots$, $44,000$ feet. The persistent contrail formation matrix (contrail matrix) at time t at level l is defined as

$$\mathbf{R}_t^l = \begin{bmatrix} r^l_{1,1,t} & r^l_{1,2,t} & \cdots & r^l_{1,451,t} \\ \vdots & \vdots & \ddots & \vdots \\ r^l_{337,1,t} & r^l_{337,2,t} & \cdots & r^l_{337,451,t} \end{bmatrix}, \tag{5}$$

where $r^l_{i,j,t}$ is 1 if $r_{contr} \leq RHw < 100\%$ and $RHi \geq 100\%$ at grid (i, j), and 0 if the conditions are not met. The Center contrail frequency indices of twenty U.S. air traffic control centers at time t at level l are defined as

$$C_{center,l,t} = \sum_{i=1}^{337} \sum_{j=1}^{451} r^l_{i,j,t} a^l_{i,j,t} c_{i,j}, \tag{6}$$

where $a^l_{i,j,t}$ is the number of aircraft within RUC 13km grid (i, j) flying closest to altitude level l at time t, and $c_{i,j}$ is 1 when grid (i, j) is inside the center and 0 if not. The twenty U.S. air traffic control centers

are listed in Table 1. The aircraft data were provided by the Federal Aviation Administration's Aircraft Situation Display to Industry (ASDI) data.

Table 1. Center index of twenty continental U.S. air traffic control centers.

Index	Name	Index	Name
1	Seattle Center (ZSE)	11	Chicago Center (ZAU)
2	Oakland Center (ZOA)	12	Indianapolis Center (ZID)
3	Los Angeles Center (ZLA)	13	Memphis Center (ZME)
4	Salt Lake City Center (ZLC)	14	Cleveland Center (ZOB)
5	Denver Center (ZDV)	15	Washington D. C. Center (ZDC)
6	Albuquerque Center (ZAB)	16	Atlanta Center (ZTL)
7	Minneapolis Center (ZMP)	17	Jacksonville Center (ZJX)
8	Kansas City Center (ZKC)	18	Miami Center (ZMA)
9	Dallas/Fort Worth Center (ZFW)	19	Boston Center (ZBW)
10	Houston Center (ZHU)	20	New York Center (ZNY)

For planning contrail reduction strategies, traffic flow managers need to know potentially high contrail regions in the next few hours. Therefore predicted contrail frequency indices are needed for contrail reduction strategies. Similar to the concept of Weather Impacted Traffic Index (WITI) introduced by Callaham et al.[18] and Sridhar,[19] and the three-dimensional index derived by Chen,[20] predicted contrail frequency index was defined as a convolution of predicted traffic data and forecast of atmospheric conditions. The index consists of the RUC forecast data and the predicted aircraft locations when t is a future time. The Center contrail frequency index can then be rewritten as

$$C_{center,l,t} = \begin{cases} \sum_{i=1}^{337} \sum_{j=1}^{451} r^l_{i,j,t} a^l_{i,j,t} c_{i,j} & \text{if } t <= t_{now}, \\ \sum_{i=1}^{337} \sum_{j=1}^{451} \hat{r}^l_{i,j,t} \hat{a}^l_{i,j,t} c_{i,j} & \text{if } t > t_{now}, \end{cases} \tag{7}$$

where t_{now} is the current time, $\hat{r}^l_{i,j}$ is defined in (5) with RUC forecast data, and $\hat{a}^l_{i,j}$ is the predicted number of aircraft within RUC 13km grid (i, j) flying closest to altitude level l at time t.

Figure 2 illustrates how contrail frequency index is computed. The aircraft trajectories and contrail formations between 33,000 feet and 34,999 feet for the hour of 8AM EDT on April 23, 2010 are shown in Fig. 2a. An one-minute time interval is used. The blue polygons indicate the contrail favorable regions; grey dots are the aircraft between 33,000 feet and 34,999 feet. When the aircraft enter the blue polygons, contrails would form as indicated by blue dots. The number of blue dots is defined as the contrail frequency index. As shown in Fig. 2b, there are 148 blue dots for the hour in Kansas City Center. Therefore, the center contrail frequency index for Kansas City Center for the hour of 8AM EDT is 148. The total time, due to all aircraft that would form contrails during the hour, is 148 minutes.

The Center contrail frequency indices for all 20 US air traffic control Centers at 34,000 feet at 8AM EDT on April 23, 2010 were computed and are shown in Fig. 3. As shown in the figure, Minneapolis Center (ZMP) and Chicago Center (ZAU) have high contrail frequency indices because there are large contrail favorable regions in the Centers and also high density of air traffic, as shown in Fig. 2a. Salt Lake City Center (ZLC) has large contrail favorable regions inside the Center but the contrail frequency index is low because not many aircraft fly through the Center. Contrail frequency index takes both atmospheric and air traffic data and quantifies the contrail activities. It will be used later in developing contrail reduction strategies.

II.C. Fuel Burn and Emission Models

The computations of aircraft fuel burn and emissions are needed in order to study the trade-offs between contrail reductions and aircraft induced emissions. This paper uses the fuel consumption model in Eurocontrols Base of Aircraft Data Revision 3.7 (BADA).[21] The air traffic data provide aircraft information including aircraft type, mass, altitude and speed to compute the fuel burn. There are five stages, climb, cruise, descent-idle, descent-approach, and descent-landing that are determined by the aircraft altitude and

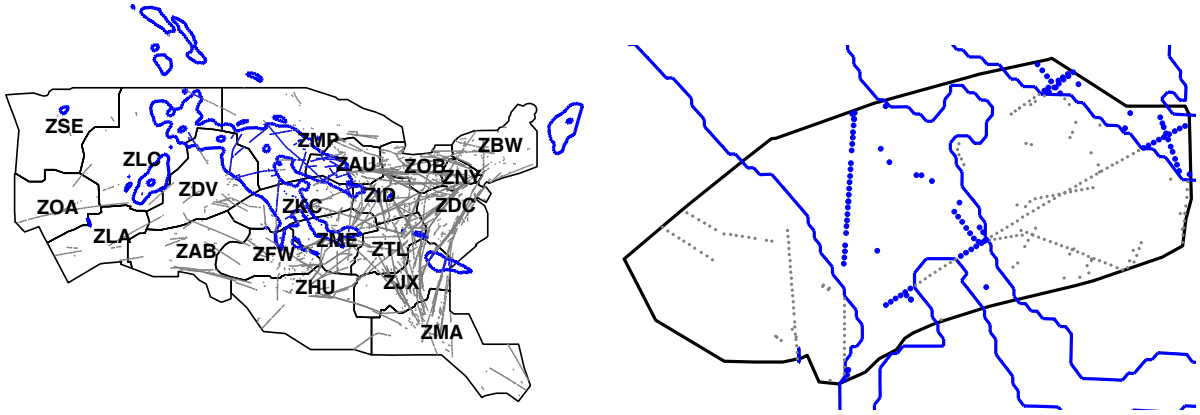

(a) entire U.S. airspace (b) Kansas City Center

Figure 2. Aircraft trajectories and contrail favorable regions at 8AM EDT on April 23, 2010.

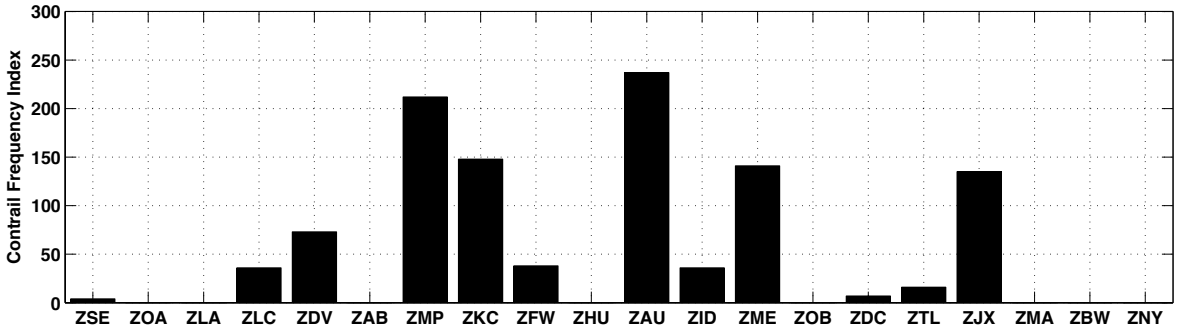

Figure 3. Center contrail frequency indices at 34,000 feet at 8AM EDT on April 23, 2010.

speed. Only climb, cruise, and descent-idle models are used in this paper since the other two are used at the low altitudes. For climb stage, the fuel burn is computed using the following equation,

$$FB = SFC \cdot T \cdot \Delta t, \tag{8}$$

where FB is the fuel burn in kilograms, SFC (kg/min·kN) is the thrust specific fuel consumption, T is the trust in Newtons, and Δt is the elapse time in minutes. For cruise, the fuel burn is

$$FB = SFC \cdot T \cdot C_{fcr} \cdot \Delta t, \tag{9}$$

where C_{fcr} is the cruise fuel flow factor. For descent-idle, the fuel burn is

$$FB = C_{f3}(1 - \frac{h}{C_{f4}}), \tag{10}$$

where C_{f3} and C_{f4} are descent fuel flow coefficients, and h is the altitude in meters. SFC in (8) and (9) are formulated as

$$\begin{aligned} \text{Jet: } SFC &= C_{f1}(1 + \frac{V_{TAS}}{C_{f2}}), \\ \text{Turboprop: } SFC &= C_{f1}(1 - \frac{V_{TAS}}{C_{f2}}) \cdot (V_{TAS}/1000), \end{aligned} \tag{11}$$

where V_{TAS} is the true air speed in meters per second, and C_{f1} and C_{f2} are thrust specific fuel consumption coefficients. The thrust in (8) for climb stage is formulated as

$$\begin{aligned} \text{Jet: } T_{climb} &= C_{Tc,1}(1 - \frac{h}{C_{Tc,2}} + C_{Tc,3} \cdot h^2), \\ \text{Turboprop: } T_{climb} &= C_{Tc,1}(1 - \frac{h}{C_{Tc,2}})/V_{TAS} + C_{Tc,3}, \end{aligned} \tag{12}$$

where $C_{Tc,1}$, $C_{Tc,2}$ and $C_{Tc,3}$ are climb thrust coefficients. For cruise, thrust is set equal to drag. Drag is computed by

$$D = \frac{C_D \cdot \rho \cdot V_{TAS}^2 \cdot S}{2}, \tag{13}$$

where D is the drag in Newtons, C_D is the drag coefficient, ρ (kg/m^3) is the air density, and S (m^2) is the wing reference area.

The emission model is based on a prototype of the Aviation Environmental Design Tool (AEDT) developed by the Federal Aviation Administration (FAA).[22] Five emissions are computed including CO_2, SO_x, CO, HC and NO_x. Emissions of CO_2 and SO_x (modeled as SO_2) are modeled based on fuel consumption.[23] The emissions are computed by

$$\begin{aligned} E_{CO_2} &= 3155 \cdot FB, \\ E_{SO_2} &= 0.8 \cdot FB, \end{aligned} \tag{14}$$

where E_{CO_2} and E_{SO_2} are emissions of CO_2 and SO_2 in grams, and FB is fuel burn in kilograms.

Emissions of CO, HC and NO_x are modeled through the use of the Boeing Fuel Flow Method 2 (BFFM2).[24] The emissions are determined by aircraft engine type, altitude, speed, and fuel burn and the coefficients in International Civil Aviation Organization (ICAO) emission data bank. In the models, fuel burn is corrected to sea-level reference temperature (273.15 K) and pressure (14.696 psi):

$$\begin{aligned} FB_c &= (FB/\delta_{amb})[\theta_{amb}^{3.8} exp(0.2M^2)], \\ \delta_{amb} &= P_{amb}/14.696, \\ \theta_{amb} &= (T_{amb} + 273.15)/273.15, \end{aligned} \tag{15}$$

where FB_c is the corrected fuel flow, P_{amb} is the at-altitude ambient pressure, T_{amb} is the at-altitude ambient temperature, and M is the Mach number. FB_c is used in ICAO emission data bank to determine the reference emission index $REIHC$, $REICO$ and $REINO_x$ for HC, CO and NO_x. The emission indices are computed by

$$\begin{aligned} EICO &= REICO(\theta_{amb}^{3.3}/\delta_{amb}^{1.02}), \\ EIHC &= REIHC(\theta_{amb}^{3.3}/\delta_{amb}^{1.02}), \\ EINO_x &= REINO_x[exp(H)](\delta_{amb}^{1.02}/\theta_{amb}^{3.3})^{0.5}, \\ H &= -19.0(\omega - 0.0063), \end{aligned} \tag{16}$$

where $EICO$, $EIHC$ and $EINO_x$ are emission indices of CO, HC and NO_x, H is the humidity correction factor, and ω is the specific humidity. The emissions are computed by

$$\begin{aligned} E_{CO} &= EICO \cdot FB, \\ E_{HC} &= EIHC \cdot FB, \\ E_{NO_x} &= EINO_x \cdot FB, \end{aligned} \tag{17}$$

where E_{CO}, E_{HC} and E_{NO_x} are emissions in grams.

III. Contrail Reduction Strategies

III.A. Use of contrail frequency index

Contrail frequency index (CFI) quantifies the contrail activities. The strategy for reducing the persistent contrail formations is to minimize contrail frequency index by altering the aircraft's cruising altitude. Assume the aircraft at altitude level l in a Center are made to fly at a different level l'. Both l and l' range from 1 to 10, corresponding to altitudes of $26,000, 28,000, \ldots, 44,000$ feet. The definition of the contrail frequency index is changed from (6) to

$$C_{center,l,t}^{l'} = \sum_{i=1}^{337} \sum_{j=1}^{451} r_{i,j,t}^{l'} a_{i,j,t}^{l} c_{i,j}, \tag{18}$$

A contrail frequency index matrix is formed as

$$\mathbf{C}_{center,t} = \begin{bmatrix} C^1_{1,t} & C^1_{2,t} & \dots & C^1_{10,t} \\ C^2_{1,t} & C^2_{2,t} & \dots & C^2_{10,t} \\ \vdots & \vdots & \ddots & \vdots \\ C^{10}_{1,t} & C^{10}_{2,t} & \dots & C^{10}_{10,t} \end{bmatrix}, \tag{19}$$

where the diagonal term $C^l_{l,t}$ is the contrail frequency index at level l before changing cruising altitude, and $C^{l'}_{l,t}$ is the contrail frequency index when guiding aircraft at level l to level l'. The contrail reduction from level l to l' is

$$\Delta C^{l'}_{l,t} = C^l_{l,t} - C^{l'}_{l,t}. \tag{20}$$

Note that when $l' > l$, not all aircraft have the ability to fly from level l to level l'. If altitude level l' is higher than an aircraft's maximal flight altitude, it stays at level l and is not counted in $C^{l'}_{l,t}$. In addition, if an aircraft crosses a sector boundary and causes congestion, it stays at level l and does not add to $C^{l'}_{l,t}$. Additional conditions can be added to satisfy other operational procedures.

The strategy is to find the altitude that would form least contrails. In other words, find the smallest element in each column of $\mathbf{C}_{center,t}$. If the aircraft are limited to alter Δl levels, the solution is the smallest element in $[C^{l-\Delta l}_{l,t} \dots C^l_{l,t} \dots C^{l+\Delta l}_{l,t}]^T$ in each column. The solution is denoted as $[\hat{l}_1 \dots \hat{l}_{10}]$. Each $\hat{l}_i$ means aircraft at flight level i is flying at level $\hat{l}_i$. If $\hat{l}_i = i$, the aircraft at level i do not alter. The total contrail reduction at the given center at time t can be expressed as

$$\Sigma\Delta C_t = \sum_{i=1}^{10} \Delta C^{\hat{l}_i}_{i,t}. \tag{21}$$

Consider the traffic situation at Kansas City Center. For $\Delta l = 2$, the CFI matrix at 8AM EDT on April 23, 2010 was computed,

$$\mathbf{C}_{ZKC} = \begin{bmatrix} \mathbf{0} & 0 & 0 & \times & \times & \times & \times & \times & \times & \times \\ 0 & \mathbf{0} & 0 & 0 & \times & \times & \times & \times & \times & \times \\ 0 & 0 & \mathbf{0} & 0 & 0 & \times & \times & \times & \times & \times \\ \times & 0 & 0 & \mathbf{0} & 0 & 0 & \times & \times & \times & \times \\ \times & \times & 61 & 89 & \mathbf{148} & 387 & 233 & \times & \times & \times \\ \times & \times & \times & 35 & 102 & \mathbf{230} & 154 & 83 & \times & \times \\ \times & \times & \times & \times & 104 & 213 & \mathbf{141} & 65 & 0 & \times \\ \times & \times & \times & \times & \times & 164 & 67 & \mathbf{22} & 0 & 0 \\ \times & \times & \times & \times & \times & \times & 137 & 17 & \mathbf{0} & 0 \\ \times & \times & \times & \times & \times & \times & \times & 18 & 0 & \mathbf{0} \end{bmatrix}, \tag{22}$$

where the elements not used are marked as $\times$. The diagonal elements of the matrix show the current CFIs at various altitudes. First consider the case if the aircraft are allowed to move one level (2,000 feet) up or down to reduce contrail formation. All the aircraft between 33,000 feet and 34,999 feet (level 5) have a total CFI of 148 ($\mathbf{C}_{ZKC}(5,5) = 148$). Moving the aircraft to level 4 will result in zero CFI ($\mathbf{C}_{ZKC}(4,5) = 0$), a reduction of CFI by 148. Other contrail reduction moves include moving aircraft from level 6 to 7 (a CFI reduction of 17), 7 to 8 (a CFI reduction of 74) and 8 to 9 (a CFI reduction of 5). The solution is expressed as [1 2 3 4 4 7 8 9 9 10], resulting in a CFI reduction from 541 to 297, a 45% reduction. If the aircraft are allowed to move two levels up or down, even greater reductions can be achieved. The moves include moving aircraft from level 5 to 4, 6 to 4, 7 to 8 and 8 to 9. The solution is expressed as [1 2 3 4 4 4 8 9 9 10], resulting in a contrail reduction from 541 to 84, an 84% reduction.

The center is divided into sectors horizontally and vertically. An air traffic controller monitors traffic in each sector and maintains separation between aircraft. The number of aircraft in a sector is kept below a maximum, referred to as Monitor Alert Parameter (MAP) in the current U.S. air traffic system, to keep the controllers workload within limits.[25] The MAP is used to define the airspace capacity. The contrail reduction moves will not change the sector counts unless they cross the sector boundaries. The strategies

only allow the moves such that the aircraft count in a sector does not exceed the sector capacity after the moves. In the previous example, Kansas City Center has 15 high sectors and 11 super-high sectors. Among them, sector 31 has the highest sector count during the hour. Sector 31 has a lower bound of 37,000 feet and is on top of sector 28, 29 and 30, shown in Fig. 4. The move from level 6 (35,000-36,999 feet) to level 7

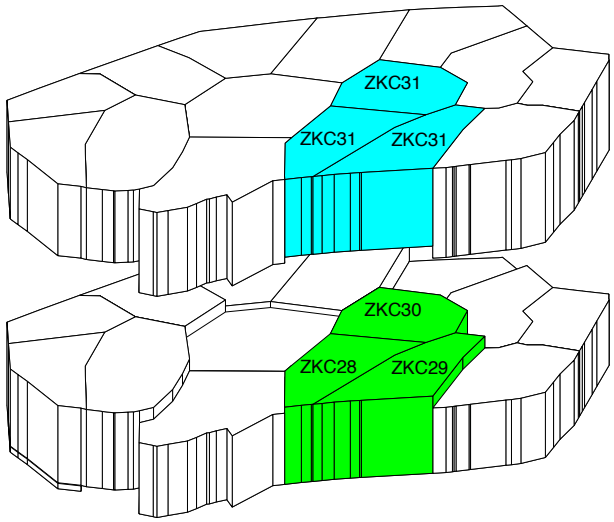

Figure 4. Kansas City Center sector 28, 29, 30 and 31.

(37,000-38,999 feet) would move some aircraft in sector 28, 29 and 30 to sector 31. Sector 28, 29, 30 and 31 have the MAP values of 18, 18, 19 and 21 respectively. Figure 5 shows the MAP values and the sector counts in sector 28, 29, 30 and 31 before and after the moves. The aircraft counts in sector 28, 29 and 30 decrease because some aircraft have been moved up to sector 31; the sector count in sector 31 increases but is still lower than the sector capacity of 21. Thus the contrail reduction moves are applied without exceeding the capacity of the airspace. The altitudes of the aircraft are changed as they enter a new Center. The number of altitude changes is not expected to result in frequent climb and descents to affect current operations. However, if needed, additional constraints can be imposed on the number of altitude changes.

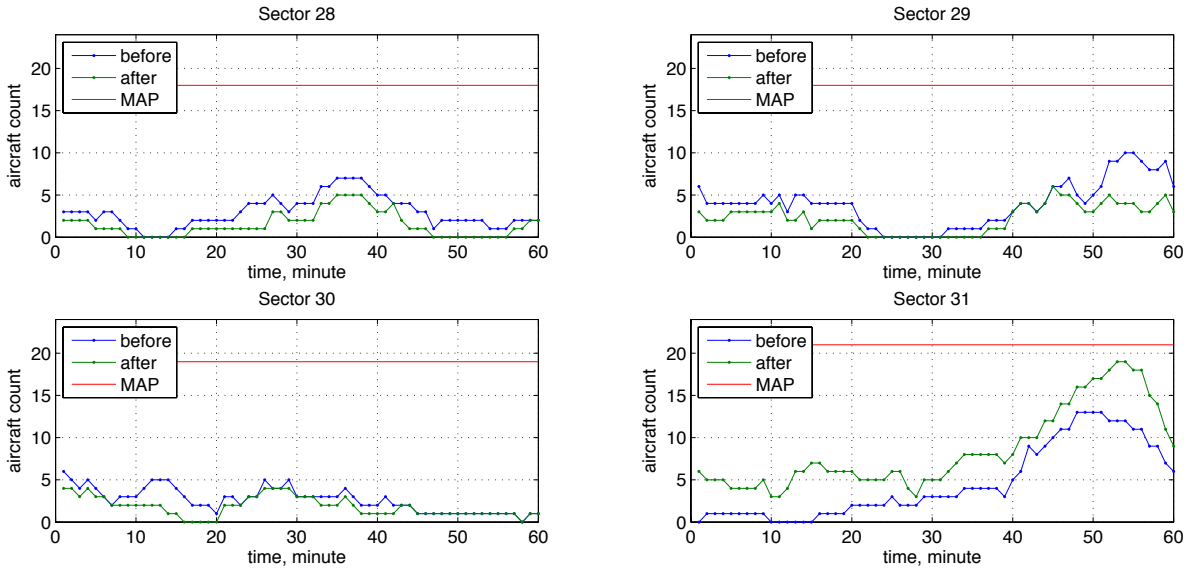

Figure 5. MAP values and sector counts before and after the contrail reduction strategies at 8AM EDT on April 23, 2010.

Data from a 24-hour period on April 23, 2010 was analyzed. The contrail reduction strategies were applied and the results are shown in Fig. 6. The center CFIs before reduction are shown in blue bars. When the aircraft altitudes are allowed to alter by 2,000 feet, the center CFIs after reduction are shown in light

blue bars. The total reduction among all centers is 62%. When the aircraft altitudes are allowed to alter by 4,000 feet, the total reduction is 88% as indicated in green bars. Since allowing aircraft to alter 4,000 feet would eliminate most of the contrail formation, the strategies in this paper limit the altitude changes to 4,000 feet.

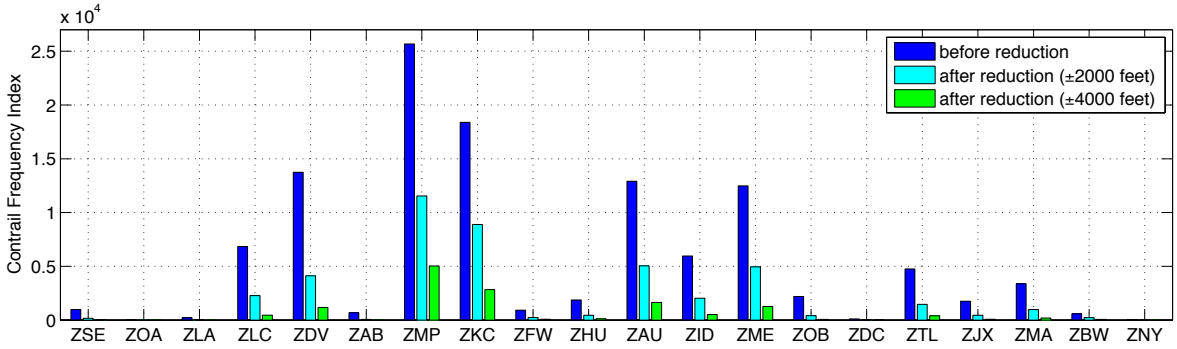

Figure 6. Results of contrail reduction strategies on April 23, 2010.

III.B. Tradeoff between contrails and emissions

Altering cruising altitudes changes the aircraft fuel consumption and emissions. In order to analyze the environmental impact of contrail reduction strategies, fuel consumption and emissions are considered in the strategies. Fuel burn and emissions computations are based on the models described in Sec.II.C. Define $E^l_{l,t}$ as the emissions for all aircraft at level l at a given center at time t before contrail reduction, and $E^{l'}_{l,t}$ as the total emissions when guiding aircraft from level l to level l'. When aircraft change their flying altitude from level l to l', the difference in emissions is

$$\Delta E^{l'}_{l,t} = E^{l'}_{l,t} - E^{l}_{l,t}. \tag{23}$$

$\Delta E^{l'}_{l,t} < 0$ implies emission reduction. Define the emission matrix as

$$\mathbf{\Delta E}_{center,t} = \begin{bmatrix} 0 & \Delta E^1_{2,t} & \dots & \Delta E^1_{9,t} & \Delta E^1_{10,t} \\ \Delta E^2_{1,t} & 0 & \dots & \Delta E^2_{9,t} & \Delta E^2_{10,t} \\ \vdots & \vdots & \ddots & \vdots & \\ \Delta E^9_{1,t} & \Delta E^9_{2,t} & \dots & 0 & \Delta E^9_{10,t} \\ \Delta E^{10}_{1,t} & \Delta E^{10}_{2,t} & \dots & \Delta E^{10}_{9,t} & 0 \end{bmatrix}. \tag{24}$$

This matrix helps to study the emissions trade-offs when applying contrail reduction strategies. For the contrail reduction solution of $[\hat{l}_1 \dots \hat{l}_{10}]$, the change in emissions can be expressed as

$$\Sigma \Delta E_t = \sum_{i=1}^{10} \Delta E^{\hat{l}_i}_{i,t}. \tag{25}$$

Consider the same example in the previous subsection and study the trade-offs between contrail reduction and CO_2 emissions. The emission matrix for CO_2 was computed based on the models described in Sec.II.C

and is the following:

$$\mathbf{\Delta E}_{ZKC} = \begin{bmatrix} \mathbf{0} & 484 & 1130 & \times & \times & \times & \times & \times & \times & \times \\ -27 & \mathbf{0} & 531 & 3562 & \times & \times & \times & \times & \times & \times \\ -41 & -31 & \mathbf{0} & 1674 & 3169 & \times & \times & \times & \times & \times \\ \times & -28 & 11 & \mathbf{0} & 1417 & 4542 & \times & \times & \times & \times \\ \times & \times & 55 & 237 & \mathbf{0} & 2143 & 3462 & \times & \times & \times \\ \times & \times & \times & 285 & 1331 & \mathbf{0} & 1683 & 1042 & \times & \times \\ \times & \times & \times & \times & 961 & 1237 & \mathbf{0} & 420 & 2 & \times \\ \times & \times & \times & \times & \times & 434 & 1892 & \mathbf{0} & 0 & 0 \\ \times & \times & \times & \times & \times & \times & 70 & 106 & \mathbf{0} & 0 \\ \times & \times & \times & \times & \times & \times & \times & 128 & 0 & \mathbf{0} \end{bmatrix}, \tag{26}$$

where the elements not used are marked as $\times$ and the unit is kilograms. As shown in the matrix and in (22), moving aircraft from level 5 to 4 results in a CFI reduction of 148 with additional CO_2 emissions of 1,417 kg ($\Delta E^4_{5,t} = 1417$); moving from level 6 to 4 results in a CFI reduction of 230 with additional CO_2 of 4,542 kg; moving from level 7 to 8 results in a CFI reduction of 74 with additional CO_2 of 1892 kg; moving from level 8 to 9 results in a CFI reduction of 5 with additional CO_2 of 106 kg. This solution achieves the most contrail frequency index reduction of 457 with additional CO_2 emissions of 7,957 kg.

Assuming the environmental impact of the contrail frequency index of 1 is equivalent to CO_2 emissions of 10 kg, the move from level 5 to 4 makes sense because a reduction of 148 in CFI is greater than the impact of additional CO_2 of 1417 kg ($148 \cdot 10 - 1417 > 0$). However, the move from level 6 to 4 is not worth while because the net impact is negative ($230 \cdot 10 - 4542 < 0$). Instead, the move from 6 to 8 is preferred because it has a CFI reduction of 66 with additional CO_2 emissions of 434 kg and reduces the net impact ($66 \cdot 10 - 434 > 0$). Similarly, the move from level 7 to 8 and from 8 to 9 are not preferred because of the net negative impacts. Aircraft at level 7 and 8 are not altered. The new solution can be denoted as [1 2 3 4 4 8 7 8 9 10], resulting in a CFI reduction of 214, with additional CO_2 emissions of 1851 kg. Compared with the maximal reduction strategy, this strategy achieves less contrail reduction, 40% versus 84%, but emits much less CO_2 emissions, $1,851$ kg vs $7,957$ kg (77% less). This example shows that the proposed contrail reduction strategies have the capability to trade off contrail reduction with emissions.

Considering the relative environment impact of emissions and contrails, the strategy would move aircraft only if the contrails reduction benefits exceed the environmental impact of additional emissions. The aircraft would be guided from level l to l' only if

$$\Delta C^{l'}_{l,t} > \frac{1}{\alpha} \Delta E^{l'}_{l,t}, \tag{27}$$

where $\Delta C_{i,t}$ and $\Delta E_{l,t}$ are defined in (20) and (23) and α is a user-defined trade-off factor. It can be interpreted as the equivalent emissions in kg that has the same environmental impact as the contrail frequency index of 1. For the maximal contrail reduction strategy, the effect of emissions is ignored. In other words, $\alpha = \infty$. Also, $\alpha = 0$ simply means no reduction strategy is applied because (27) will never be true. Higher values of α means more contrail reduction and more emissions (closer to maximal reduction strategy); lower α means less contrail reduction and less emissions (closer to no reduction). In the previous example, α is 10.

The appropriate value of α can be determined in two different ways. It is possible to monetize the value of both contrails and emissions as suggested in Ref. 26. Another approach is to consider contrails and emissions as disturbances to the global climate equilibrium and measure their impact as changes to the global mean surface temperature.[27] However, both these methods are beyond the scope of this paper and the value of α will be considered as a user-preference weighting factor in the rest of the paper.

IV. Results

This section presents the results of contrail reduction strategies and the trade-offs between contrail reduction and extra emissions over a 24-hour period on April 23, 2010. The 24-hour period starts at 4AM EDT and ends at 4AM the next day. The strategies allow aircraft to move 4,000 feet up or down within a center and use various user-defined α values to trade off between contrail reduction and emissions. This paper focuses on the trade-offs between contrails and CO_2 emissions while other emissions like NOx, SO_2, HC

and CO have a similar trend. Figure 7 shows the hourly variations in contrail reduction and extra emissions with different trade-off factors during a 24-hour period over the entire U.S. In Fig. 7a, the blue line shows the hourly CFI during the day with no reduction strategy applied ($\alpha = 0$). When reduction strategies are applied, it is consistent that higher α results in lower CFI, meaning more reduction. The maximal reduction strategy ($\alpha = \infty$), shown in the magenta line, has the lowest CFI at every hour. On the other hand, Fig. 7b shows that higher α results in higher extra CO_2 emissions, and the maximal reduction strategy has the highest CO_2 emissions. The results show that contrails reduction results in extra CO_2 emissions.

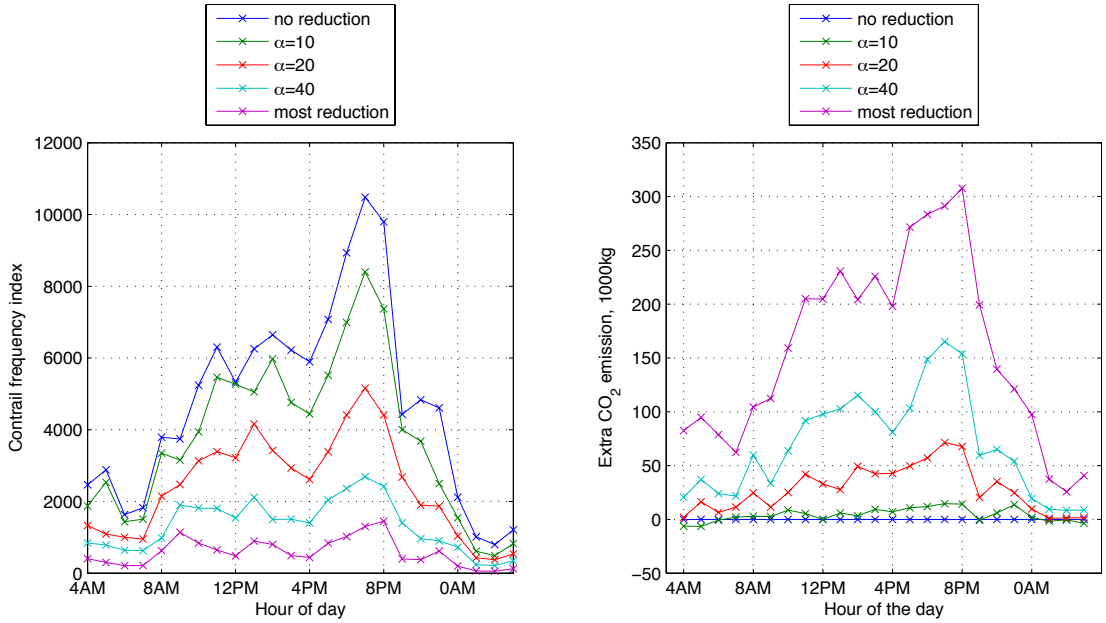

(a) contrail frequency index

(b) extra CO_2 emissions

Figure 7. Hourly contrail reduction and extra CO_2 emissions using different trade-off factors on April 23, 2010.

Looking at the Center level, Fig. 8 shows the daily contrail reduction and extra emissions in twenty U.S. air traffic control centers. The blue bars in Fig. 8a are the daily center contrail frequency index for each Center. It is consistent that for all Centers, higher α values results in more contrail reduction and the maximal reduction strategy achieves most contrail reduction in all twenty Centers. On the other hand, higher α also results in more CO_2 emissions, as shown in Fig. 8b, while the maximal reduction strategy has the most CO_2 emissions. Table 2 summarizes the trade-offs between contrail reduction and extra CO_2 emissions over the entire U.S. on April 23, 2010. On that day, the maximal reduction strategy has an 88% contrail reduction rate with extra CO_2 emissions of 3778 megagram (Mg). A smaller value of α lowers the contrail reduction ratio but has less emissions. For $\alpha = 40$, the contrail reduction rate is 73% with 2,621 Mg extra CO_2 emissions, 31% less than the emissions in the maximal reduction strategy. If CO_2 has more environmental impact, using $\alpha = 10$ results in a contrail reduction of 21% with 100 Mg extra CO_2 emissions, 97% less than the emissions in the maximal reduction strategy. As for fuel burn, considering all aircraft flying between 26,000 feet and 44,000 feet on a day with large contrail favorable regions, an 80% reduction in contrails can be achieved with around 1% extra fuel. The increase in fuel would be less on a day with smaller contrail favorable regions. The main focus of this paper is to study the trade-offs between contrail reduction and extra emissions. Therefore, the factor of the extra fuel burn is not taken into account in the strategies.

Figure 9 shows the contrail reduction versus extra CO_2 emissions with various α values. In the figure, more contrail reduction takes place from left to right and more CO_2 emissions occurs from bottom to top. At the lower-left point, no reduction strategy is applied. The upper-right point is the maximal reduction strategy. As the values of α increases, the curve moves from lower-left to upper-right. The user-defined trade-off factor α provides a flexible way to trade off between contrail reduction and extra emissions. Better understanding of the trade-offs between contrails and emissions and impact on the climate need to be

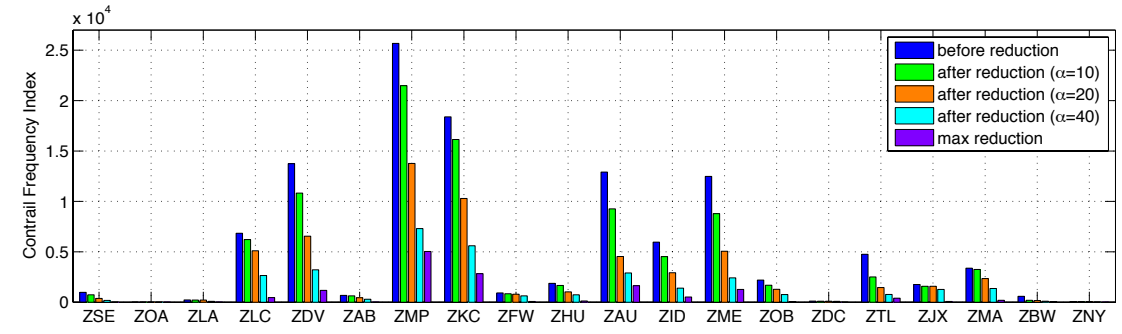

(a) contrail frequency index

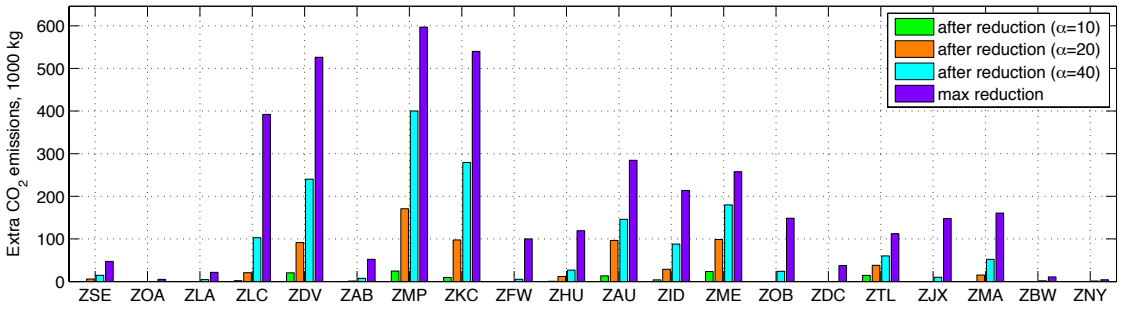

(b) extra CO_2 emissions

Figure 8. Center contrail reduction and extra CO_2 emissions using different trade-off factors on April 23, 2010.

developed to fully utilize this class of contrail reduction strategies.

Table 2. Results of contrail reduction strategies on April 23, 2010.

contrail reduction strategy	contrail reduction	extra CO_2 emissions (Mg)
max reduction	99586 (88%)	3778 (100%)
$\alpha = 80$	94976 (84%)	2621 (69%)
$\alpha = 40$	81745 (73%)	1644 (44%)
$\alpha = 20$	55457 (49%)	674 (18%)
$\alpha = 10$	22849 (21%)	100 (3%)

V. Conclusions

A class of strategies for reducing persistent contrail formations with the capability to trade off between contrails and emissions has been developed. The concept of contrail frequency index is defined and used to quantify the contrail activities. The strategy of reducing the persistent contrail formations is to minimize the contrail frequency index by altering the aircraft's cruising altitude with consideration to extra emissions. The strategies use a user-defined factor to trade off between contrail reduction and extra emissions. The analysis results show that the contrails can be reduced with extra emissions and without adding congestion to airspace. For the day tested, the results show that the maximal contrail reduction strategy can achieve a contrail reduction of 88%. When a trade-off factor is used, the strategy can still achieve a 73% contrail reduction while emitting 31% less emissions compared to the maximal contrail reduction strategy, or achieve a 21% contrail reduction while only emitting 97% less emissions. The user-defined trade-off factor provides a flexible way to trade off between contrail reduction and extra emissions. Better understanding of the trade-offs between contrails and emissions and impact on the climate need to be developed to fully utilize this class of contrail reduction strategies. The strategies provide a starting point for developing operational policies to reduce the impact of aviation on climate.

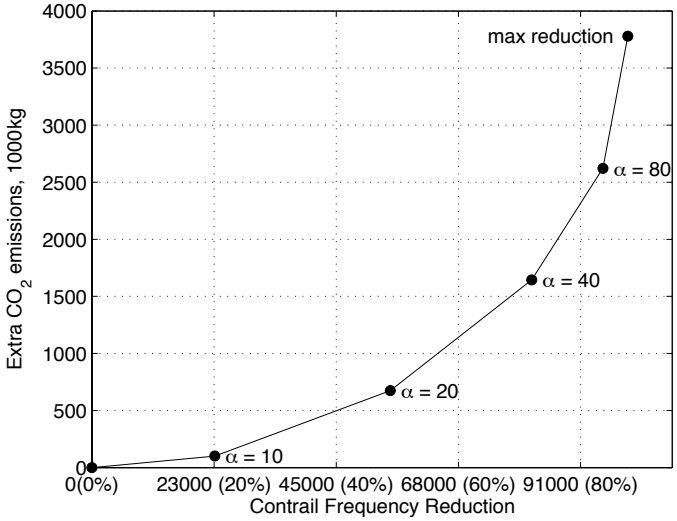

Figure 9. Contrail reduction versus extra CO_2 emissions on April 23, 2010.

References

[1]Waitz, I., Townsend, J., Cutcher-Gershenfeld, J., Greitzer, E., and Kerrebrock, J., "Report to the United States Congress: Aviation and the Environment, A National Vision, Framework for Goals and Recommended Actions," Tech. rep., Partnership for AiR Transportation Noise and Emissions Reduction, London, UK, December 2004.

[2]Meerkotter, R., Schumann, U., Doelling, D. R., Minnis, P., Nakajima, T., and Tsushima, Y., "Radiative forcing by contrails," *Annales Geophysicae*, Vol. 17, 1999, pp. 1080–1094.

[3]Marquart, S., Ponater, M., Mager, F., and Sausen, R., "Future Development of Contrail Cover, Optical Depth, and Radiative Forcing: Impacts of Increasing Air Traffic and Climate Change," *Journal of Climate*, Vol. 16, September 2003, pp. 2890–2904.

[4]"The Environmental Effects of Civil Aircraft in Flight," Tech. rep., Royal Commission on Environmental Pollution, London, UK, 2002.

[5]Mannstein, H. and Schumann, U., "Aircraft induced contrail cirrus over Europe," *Meteorologische Zeitschrift*, Vol. 14, No. 4, 2005, pp. 549–554.

[6]Gierens, K., Limb, L., and Eleftheratos, K., "A Review of Various Strategies for Contrail Avoidance," *The Open Atmospheric Science Journal*, Vol. 2, 2008, pp. 1–7.

[7]Noppel., F. and Singh, R., "Overview on Contrail and Cirrus Cloud Avoidance Technology," *Journal of Aircraft*, Vol. 44, No. 5, 2007, pp. 1721–1726.

[8]Mannstein, H., Spichtinger, P., and Gierens, K., "A note on how to avoid contrail cirrus," *Transportation Research. Part D, Transport and environment*, Vol. 10, No. 5, September 2005, pp. 421–426.

[9]Campbell1, S. E., Neogi, N. A., and Bragg, M. B., "An Optimal Strategy for Persistent Contrail Avoidance," *AIAA Guidance, Navigation and Control Conference*, AIAA-2008-6515, AIAA, Honolulu, HI, August 2008.

[10]Fichter, C., Marquart, S., Sausen, R., and Lee, D. S., "The impact of cruise altitude on contrails and related radiative forcing," *Meteorologische Zeitschrift*, Vol. 14, No. 4, August 2005, pp. 563–572.

[11]Williams, V., Noland, R. B., and Toumi, R., "Reducing the climate change impacts of aviation by restricting cruise altitudes," *Transportation Research. Part D, Transport and environment*, Vol. 7, No. 5, November 2002, pp. 451–464.

[12]Williams, V. and Noland, R. B., "Variability of contrail formation conditions and the implications for policies to reduce the climate impacts of aviation," *Transportation Research. Part D, Transport and environment*, Vol. 10, No. 4, July 2005, pp. 269–280.

[13]Ponater, M., Marquart, S., and Sausen, R., "Contrails in a Comprehensive Global Climate Model: Parameterization and Radiative Forcing Results," *Journal of Geophysical Research*, Vol. 107, No. D13, 2002, pp. ACL 2–1.

[14]Gierens, K. M., Schumann, U., Smit, H. G. J., Helten, M., and Zangl1, G., "Determination of humidity and temperature fluctuations based on MOZAIC data and parametrisation of persistent contrail coverage for general circulation models," *Annales Geophysicae*, Vol. 15, 1997, pp. 1057–1066.

[15]Duda, D. P., Minnis, P., Costulis, P. K., and Palikonda, R., "CONUS Contrail Frequency Estimated from RUC and Flight Track Data," *European Conference on Aviation, Atmosphere, and Climate*, Friedrichshafen at Lake Constance, Germany, June-July 2003.

[16]Alduchov, O. A. and Eskridge, R. E., "Improved Magnus Form Approximation of Saturation Vapor Pressure," *Journal of Applied Meteorology*, Vol. 35, No. 4, April 1996, pp. 601–609.

[17]Chen, N. Y., Sridhar, B., and Ng, H. K., "Prediction and Use of Contrail Frequency Index for Contrail Reduction Strategies," *AIAA Guidance, Navigation, and Control Conference*, Toronto, Ontario, August 2010.

[18]Callaham, M. B., DeArmon, J. S., Cooper, A., Goodfriend, J. H., Moch-Mooney, D., and Solomos, G., "Assessing NAS Performance: Normalizing for the Effects of Weather," *4th USA/Europe Air Traffic Management R&D Symposium*, Santa Fe, NM, December 2001.

[19]Sridhar, B. and Swei, S., "Relationship between Weather, Traffic and Delay Based on Empirical Methods," *6th AIAA Aviation Technology, Integration and Operations Conference (ATIO)*, Wichita, KS, September 2006.

[20]Chen, N. Y. and Sridhar, B., "Estimation of Air Traffic Delay Using Three Dimensional Weather Information," *8th AIAA Aviation Technology, Integration and Operations Conference (ATIO)*, Anchrorage, AK, September 2008.

[21]EUROCONTROL Validation Infrastructure Centre of Expertise, France, *User manual for the base of aircraft data (BADA)*, 3rd ed., March 2009.

[22]Federal Aviation Administration, Washington, DC, *Aviation Environmental Design Tool (AEDT) User Guide: Beta1c*, October 2010.

[23]Hadaller, O. J. and Momenthy, A. M., "The Characteristics of Future Fuels," Project Report D6-54940, Boeing publication, 1989.

[24]Baughcuma, S., Tritz, T., Henderson, S., and Pickett, D., "Scheduled Civil Aircraft Emission Inventories for 1992: Database Development and Analysis," Project Report NASA CR 4700, April 1996.

[25]Sridhar, B., Kulkarni, D., and Sheth, K., "Impact of Uncertainty on the Prediction of Airspace Complexity of Congested Sectors," *Air Traffic Control Quarterly*, Vol. 19, No. 1, 2011, pp. 1–23.

[26]ONeill, M., Dumont, J., Reynolds, T., and Hansman, J., "Methods for Evaluating Environmental and Performance Tradeoffs for Air Transportation Systems," *11th AIAA Aviation Technology, Integration and Operations Conference (ATIO)*, Virginia Beach, VA, September 2011.

[27]Fuglestvedta, J., Shineb, K., Berntsen, T., Cook, J., Lee, D., Stenke, A., Skeie, R., Velders, G., and Waitz, I., "Transport impacts on atmosphere and climate: Metrics," *Atmospheric Environment*, Vol. 44, No. 37, December 2010, pp. 4648–4677.